# Formation of Porous Anodic Titanium Oxide Films in Hot Phosphate/Glycerol Electrolyte

H. Habazaki[1]*, M. Teraoka, Y. Aoki, P. Skeldon# and G.E. Thompson#

Graduate School of Engineering, Hokkaido University, N13-W8, Sapporo 060-8628, Japan

#Corrosion and Protection Centre, School of Materials, The University of Manchester, P.O. Box 88, Manchester, M60 1QD, UK

*Corresponding author; phone & fax +81-11-706-6575, e-mail address habazaki@eng.hokudai.ac.jp

[1] ISE member

The present study reveals the formation of porous anodic films on titanium at an increased growth rate in hot phosphate/glycerol electrolyte by reducing the water content. A porous titanium oxide film of 12 μm thickness, with a relatively low content of phosphorus species, is developed after anodizing at 5 V for 3.6 ks in 0.6 mol $dm^{-3}$ $K_2HPO_4$+0.2 mol $dm^{-3}$ $K_3PO_4$/glycerol electrolyte containing only 0.04% water at 433 K. The growth efficiency is reduced by increasing the formation voltage to 20 V, due to formation of crystalline oxide, which induces gas generation during anodizing. The film formed at 20 V consists of two layers, with an increased concentration of phosphorus species in the inner layer. The outer layer, comprising approximately 25% of the film thickness, is developed at low formation voltages, of less than 10 V, during the initial anodizing at a constant current density of 250 A $m^{-2}$. The pore diameter is not significantly dependent upon the formation voltage, being ~10 nm.

Keywords; anodizing, organic electrolyte, titanium oxide, porous anodic oxide, crystallization

## 1. Introduction

Self-organized porous anodic titanium oxide films have attracted much attention mainly due to their wide potential applications, including dye-sensitized solar cells [1-3], photocatalysis [4-11], self-cleaning, electrochromism, sensors [12-14] and biomedical application [15]. The porous anodic titanium oxide films, usually with nanotubular structures, are formed in fluoride-containing

electrolytes [16, 17]. Fluoride-free hot phosphate/glycerol electrolyte is also useful to develop porous anodic films on various valve metals, including aluminium, niobium, titanium and tantalum [18-21]. The anodic film formed on titanium in such an electrolyte was relatively thin (only ~300 nm) [20], and the efficiency for film formation was low due to gas evolution [22]. The gas evolution is associated with the development of crystalline oxide in growing anodic titanium oxide [23, 24]. Thus, inhibition of crystalline oxide formation is essential to form thick porous anodic titanium oxide in hot phosphate/glycerol electrolyte at an improved efficiency.

It has recently been reported that the water content in the phosphate/glycerol electrolyte influences significantly the growth rate and composition of the porous films formed on niobium [21]. When the water content in the electrolyte is reduced to 0.08 mass%, the growth rate of the anodic film at a formation voltage of 10 V is markedly enhanced. Further, phosphate anions are incorporated into the anodic films during anodizing in the electrolyte of reduced water content, whereas an anodic film that is practically free from phosphate is developed in the electrolyte containing 0.2 mass% or higher water contents. In general, the incorporation of foreign species in anodic oxides impedes an amorphous-to-crystalline transition [25-27].

In the present study, titanium has been anodized in phosphate/glycerol electrolyte with reduced water content to grow relatively thick porous anodic titanium oxide films. Thick porous anodic titanium oxide films are suitable for many applications, including photocatalysis and dye-sensitized solar cells due to the increased available surface area.

## 2. Experimental

The specimens used for anodizing were prepared from 99.5% pure titanium sheet of 0.5 mm thickness. Prior to anodizing, the specimens were electropolished in 1 mol $dm^{-3}$ NaCl/ethylene glycol solution at 293 K at 20 V for 200 s and subsequently at 5 V for 600 s [28]. The electropolished specimens were anodized at 5 and 20 V in stirred glycerol electrolyte containing 0.6 mol $dm^{-3}$ $K_2HPO_4$ and 0.2 mol $dm^{-3}$ $K_3PO_4$ at 433 K under a nitrogen atmosphere. The water content in the electrolyte was 0.04 or 0.1 mass%. A constant current density of 250 A $m^{-2}$ was applied before reaching the selected formation voltage. A platinum sheet was used as a counter electrode.

Surfaces and cross-sections of the anodized specimens were observed using a JEOL JSM-6500F or JSM-6610 scanning electron microscope operated at 10 kV. Depth profiles of the anodized specimens were obtained by GDOES, using a Jobin-Yvon 5000 RF instrument, in an argon atmosphere of 600 Pa with application of RF of 13.56 MHz and power of 50 W. Light emissions of characteristic wavelengths were monitored throughout the analysis with a sampling time of 0.01 s to obtain depth profiles. The wavelengths of the spectral lines used were 365.350, 178.287, 130.217 and 165.701 nm for titanium, phosphorus, oxygen and carbon respectively. The signals were detected from a circular area of approximately 4 mm diameter. In order to estimate the pore size in the anodic films, nitrogen gas adsorption/desorption isotherms were measured at 77 K using a Bel Japan, Belsorp-mini instrument. The pore size distribution was analyzed using BJH method [29], which is useful for

mesopores in the range of 2 to 50 nm size. The structure of the anodic films was identified by X-ray diffraction (Rigaku, RINT-2000) using Cu Kα radiation.

## 3. Results and Discussion

Fig. 1 shows the voltage and current transients during anodizing of titanium in hot phosphate/glycerol electrolytes containing 0.04 and 0.1% water at formation voltages of 5 and 20 V for 3.6 ks (Figs. 1(a) and (c)), with the initial transients for 300 s disclosing in Figs. 1(b) and (d). In the electrolyte containing 0.1% water, the formation voltages of 5 or 20 V are more rapidly attained during the initial period of anodizing at a constant current density of 250 A $m^{-2}$, while the voltage rise is delayed in the electrolyte containing 0.04% water (Figs. 1(b) and (d)). In the electrolyte with reduced water content, the formation voltage reaches 5 and 20 V after anodizing for 90 and 225 s, respectively. During initial anodizing at the constant current density, the voltage of ~3.6 V is maintained for 80~90 s after initial voltage surge to approximately 5 V. Then, the voltage suddenly increases to the selected formation voltage of 5 V or to ~8.8 V when the selected formation voltage is 20 V. In the latter case, the formation voltage of 8-9 V continues to ~180 s, followed by gradual increase in the formation voltage to 20 V. As shown later, the porous anodic oxide film was formed during the constant current anodizing. The sudden voltage increase from ~3.6 V to 5 or ~8.8 V and gradual increase from 8-9 V to 20 V may be associated with the change in the composition of electrolyte at the pore base, which causes the thickness and/or composition of the barrier layer, sandwiched by the porous layer and metal

substrate. In this alkaline organic electrolyte, the formation of titanium oxide should reduce the $OH^-$ ions by the following reaction.

$$Ti + 4OH^- \rightarrow TiO_2 + 2H_2O + 4e^-$$

The reduced alkaline nature at the pore base may be one of the reasons for the increase in the formation voltage by thickening of the barrier layer and/or increased resistivity of the barrier layer. Further detailed understanding is the subject of future study.

During anodizing at constant voltages, the current density increases by two orders of magnitude at 5 V or one order of magnitude at 20 V by reducing the water content. Thus, a significant influence of the water content is evident during anodizing of titanium, as in the growth of anodic niobium oxide [21]. Since only very thin anodic oxide films, less than 300 nm thickness, were developed in the electrolyte containing 0.1% water, the characterization of the anodic films have been carried out only for the specimens anodized in the electrolyte containing 0.04% water.

Associated with the increased current density by reducing the water content, relatively thick anodic oxide films are formed in the electrolyte containing 0.04% water. Fig. 2 reveals cross-sectional SEM observations of the anodic films formed in the electrolyte with reduced water content. From the inset images in Figs. 2a and 2b, the formation of anodic films of 12 and 2.1 μm thickness at 5 and 20 V, respectively, is evident. The porous nature of the anodic films is disclosed in the high magnification images of the outer regions of the anodic films. In the anodic film formed at 5 V, the outer part of the film, ~360 nm thick, has finer pores, compared with the underlying film (Fig. 2a). The outer layer may

be formed prior to attaining the selected voltage of 5 V, when formation of a porous film with finer pore morphology is anticipated. The formation of cylindrical pores, oriented approximately normal to the film/electrolyte interface, is evident in Fig. 2b. The pore size is apparently 10 nm or less. The backscattered electron image (the inset) reveals that the anodic film formed at 20 V consists of two layers. The inner layer, 1.6 μm thick, has a light appearance, which is associated with increased incorporation of phosphorus species in the inner layer, as shown later. Due to atomic number contrast, the inner layer containing light phosphorus species has a light appearance.

Since the pore size is not clearly identified by SEM observations, the pore size distribution has been examined using nitrogen gas adsorption at 77 K. Fig. 3 shows the pore size distributions obtained from nitrogen adsorption isotherms. In this Figure, $V_p$ denotes the pore volume and $R_p$ is the pore radius. The pore size distributions of the anodic films formed at 5 and 20 V are similar and reveal no significant dependence on the formation voltage. The peak pore radius obtained from the nitrogen gas adsorption is 6 nm, being approximately in agreement with the SEM observation (Fig. 2). From the pore size distribution, the pore radius is in the range of 3 to 8 nm throughout the film thickness for both the anodic films. Although the pore sizes of the outer and inner layers appear to be different from SEM observations, there is no significant difference in the pore size distributions for the anodic oxide films formed at 5 and 20 V. This is in contrast to porous anodic alumina films formed in aqueous acid electrolytes, in which pore size increases with the rise of formation voltage [30]. Nanotube diameter of the anodic $TiO_2$ nanotube films formed in fluoride electrolyte also increases linearly with the

formation voltage, with the value increasing from 30 nm at 5 V to 100 nm at 20 V [17]. Since a small pore size of ~10 nm is formed in the present electrolyte even at 20 V, the present electrolyte is suitable to form porous films with pores as small as ~10 nm in diameter.

In contrast to the pore size, the composition of the anodic films is dependent upon the formation voltage. GDOES depth profiles of the anodic film formed at 5 V (Fig. 4a) and 20 V (Fig. 4b) disclose that the films formed on titanium contain low concentrations of carbon species and oxide-based films are developed in the present organic electrolyte. The oxygen source to form anodic films should be the water impurity in the electrolyte [21]. The phosphate is incorporated into the anodic films, but the incorporation is dependent upon the formation voltage; relatively high phosphorus incorporation occurs only in the inner layer of the anodic film formed at 20 V. The sputtering time of the outer layer with relatively low phosphorus concentration is 10 s, which is 25% of the total sputtering time of the anodic oxide film. This ratio is approximately in agreement with the relative thickness of the outer layer found in the inset SEM cross-sectional image shown in Fig. 2b. The formation of the inner layer enriched on phosphorus species during constant voltage anodizing was confirmed from the absence of phosphorus-enriched layer in the anodic film that formed by anodizing to 20 V without holding the voltage. The phosphorus content in the inner layer, examined by EDS, was ~6 at% ([P]/([Ti]+[P])). In the film formed at 5 V, only ~2 at% phosphorus was incorporated. The phosphorus-incorporated $TiO_2$ is of interest as a photocatalyst under visible-light irradiation [31].

A thicker film is developed at 5 V after anodizing for 3.6 ks, compared with the film formed

at 20 V (Fig. 2). Fig. 5 shows the change in film thickness with charge passed during anodizing at 5 and 20 V. The thicknesses of the anodic oxide films were measured by cross-sectional SEM observations after anodizing for several periods of anodizing time. It is obvious from this figure that the growth rate is higher at 5 V than at 20 V. At both formation voltages, the anodic films thicken linearly with charge passed during anodizing, suggesting that growth efficiency is unchanged during anodizing. The rate of film growth at 20 V was 5.5 x $10^{-12}$ m $C^{-1}$ $m^2$, which increased to 2.3 x $10^{-11}$ m $C^{-1}$ $m^2$ at 5 V. Assuming this growth rate at 5 V, the thickness of the anodic oxide film formed during initial anodizing at a constant current density of 50 A $m^{-2}$ for 90 s is 0.5 μm, which is slightly thicker than the outer layer observed by SEM (Fig. 2a). The growth rate during the initial anodizing at the constant current density may be lower than that after reaching 5 V.

The reduced growth rate at 20 V is associated with the formation of crystalline oxide. The X-ray diffraction pattern of titanium anodized at 5 V showed only broad diffraction peaks, other than the intense substrate peaks, indicating a poorly crystalline nature of the anodic oxide (Fig. 6). In contrast, sharp peaks due to the presence of anatase appeared in the pattern of titanium anodized at 20 V. The formation of crystalline oxide induces gas generation during anodizing [22-24], such that the efficiency of film growth is reduced.

In this manner, micrometer-thick nanoporous anodic oxide films are developed on titanium by reducing water content in hot phosphate-glycerol electrolyte. In contrast to the formation of anodic titanium oxide nanotube layers in fluoride-containing electrolytes [16, 17], the present fluoride-free

electrolyte provides nanoporous anodic films. Findings indicate that the formation of titanium oxide nanotube or nanoporous layer is dependent upon the conditions of anodizing, not typical in Ti/anodic titanium oxide system. In the present electrolyte, pore size is not dependent upon the formation voltage, in contrast to the increase in pore size of porous anodic alumina and titanium oxide nanotube films. The mechanism of the present anodic nanoporous oxide films on titanium may be somewhat different from that of usual porous and nanotube films in aqueous electrolytes. This is the subject of further study.

## 4. Conclusions

Thick anodic titanium oxide films can be formed on commercially pure titanium in hot phosphate/glycerol electrolyte by reducing the water content in the electrolyte. A 12 μm-thick anodic film is formed by anodizing at 5 V for 3.6 ks, contrasting with a thickness of 2.1 μm for formation at 20 V. The reduced thickness as a result of increasing the formation voltage is associated with crystallization of the anodic oxide, which induces gas generation during anodizing. The pore diameter is not significantly dependent upon the formation voltage, being ~6 nm and 10-12 nm in the outer and inner regions of the films respectively. The outer layer is formed at low formation voltages before reaching the selected voltage.

Acknowledgments

The present work was supported in part by Grants-in-Aid for Scientific Research (A) No. 19206077 and for Exploratory Research, No.21656180 from the Japan Society for the Promotion of Science as well as by the Global COE Program (Project No. B01: Catalysis as the Basis for Innovation in Materials Science) from the Ministry of Education, Culture, Sports, Science and Technology, Japan.

References

[1] G.K. Mor, K. Shankar, M. Paulose, O.K. Varghese, C.A. Grimes, Nano Lett., 6 (2006) 215.

[2] M. Paulose, K. Shankar, O.K. Varghese, G.K. Mor, C.A. Grimes, J. Phys. D: Appl. Phys., 39 (2006) 2498.

[3] K. Shankar, G.K. Mor, H.E. Prakasam, S. Yoriya, M. Paulose, O.K. Varghese, C.A. Grimes, Nanotechnol., 18 (2007)

[4] G.K. Mor, K. Shankar, O.K. Varghese, C.A. Grimes, J. Mater. Res., 19 (2004) 2989.

[5] X. Quan, S.G. Yang, X.L. Ruan, H.M. Zhao, Environ. Sci. Technol., 39 (2005) 3770.

[6] M. Paulose, K. Shankar, O.K. Varghese, G.K. Mor, B. Hardin, C.A. Grimes, Nanotechnol., 17 (2006) 1446.

[7] G.K. Mor, K. Shankar, M. Paulose, O.K. Varghese, C.A. Grimes, Nano Lett., 5 (2005) 191.

[8] C.K. Varghese, M. Paulose, K. Shankar, G.K. Mor, C.A. Grimes, J. Nanosci. Nanotechnol., 5 (2005) 1158.

[9] A. Ghicov, J.M. Macak, H. Tsuchiya, J. Kunze, V. Haeublein, L. Frey, P. Schmuki, Nano Lett., 6 (2006) 1080.

[10] Y.K. Lai, L. Sun, Y.C. Chen, H.F. Zhuang, C.J. Lin, J.W. Chin, J. Electrochem. Soc., 153 (2006) D123.

[11] J.M. Macak, A. Ghicov, R. Hahn, H. Tsuchiya, P. Schmuki, J. Mater. Res., 21 (2006) 2824.

[12] O.K. Varghese, D.W. Gong, M. Paulose, K.G. Ong, C.A. Grimes, Sens. Actuators B, 93 (2003) 338.

[13] M. Paulose, O.K. Varghese, G.K. Mor, C.A. Grimes, K.G. Ong, Nanotechnol., 17 (2006) 398.

[14] P. Xiao, B.B. Garcia, Q. Guo, D.W. Liu, G.Z. Cao, Electrochem. Commun., 9 (2007) 2441.

[15] H. Tsuchiya, J.M. Macak, L. Muller, J. Kunze, F. Muller, P. Greil, S. Virtanen, P. Schmuki, J. Biomed. Mater. Res. Part A, 77A (2006) 534.

[16] V. Zwilling, E. Darque-Ceretti, A. Boutry-Forveille, D. David, M.Y. Perrin, M. Aucouturier, Surf. Interface Anal., 27 (1999) 629.

[17] A. Ghicov, P. Schmuki, Chem. Commun., (2009) 2791.

[18] Q. Lu, G. Alcala, P. Skeldon, G.E. Thompson, M.J. Graham, D. Masheder, K. Shimizu, H. Habazaki, Electrochim. Acta, 48 (2002) 37.

[19] Q. Lu, T. Hashimoto, P. Skeldon, G.E. Thompson, H. Habazaki, K. Shimizu, Electrochemical and Solid-State Letters, 8 (2005) B17.

[20] Q. Lu, J. Alberch, T. Hashimoto, S.J. Garcia-Vergara, H. Habazaki, P. Skeldon, G.E. Thompson, Corros. Sci., 50 (2008) 548.

[21] H. Habazaki, Y. Oikawa, K. Fushimi, Y. Aoki, K. Shimizu, P. Skeldon, G.E. Thompson, Electrochim. Acta, 54 (2009) 946.

[22] H. Habazaki, Y. Oikawa, K. Fushimi, K. Shimizu, S. Nagata, P. Skeldon, G.E. Thompson, Electrochim. Acta, 53 (2007) 1775.

[23] C.K. Dyer, J.S.L. Leach, J. Electrochem. Soc., 125 (1978) 1032.

[24] H. Habazaki, M. Uozumi, H. Konno, K. Shimizu, P. Skeldon, G.E. Thompson, Corros. Sci., 45 (2003) 2063.

[25] K. Shimizu, G.E. Thompson, G.C. Wood, Thin Solid Films, 77 (1981) 313.

[26] H. Habazaki, K. Shimizu, S. Nagata, P. Skeldon, G.E. Thompson, G.C. Wood, Corros. Sci., 44 (2002) 1047.

[27] H. Habazaki, T. Ogasawara, H. Konno, K. Shimizu, S. Nagata, P. Skeldon, G.E. Thompson, Corros. Sci., 49 (2007) 580.

[28] K. Fushimi, H. Habazaki, Electrochim. Acta, 53 (2008) 3371.

[29] E.P. Barrett, L.G. Joyner, P.H. Halenda, J. Am. Chem. Soc., 73 (1951) 373.

[30] K. Ebihara, H. Takahashi, M. Nagayama, J. Surf. Finish. Soc. Jpn., 33 (1982) 156.

[31] R.Y. Zheng, L. Lin, J.L. Xie, Y.X. Zhu, Y.C. Me, J. Phys. Chem. C, 112 (2008) 15502.

Figure captions

Fig. 1 Voltage-time and current-time responses of titanium during anodizing at (a), (b) 5 V and (c), (d) 20 V in 0.6 mol $d^{-3}$ $K_2HPO_4$+0.2 mol $dm^{-3}$ $K_3PO_4$ glycerol electrolytes containing 0.04 and 0.1 mass% water at 433 K for 3.6 ks. Constant current density of 250 A $m^{-2}$ was applied before reaching the selected voltages.

Fig. 2 Scanning electron micrographs of fractured cross-sections of the anodic films formed on titanium at 5 V (outer part (a) and inner part (b)) and 20 V (outer part (c)) in 0.6 mol $d^{-3}$ $K_2HPO_4$+0.2 mol $dm^{-3}$ $K_3PO_4$ glycerol electrolyte containing 0.04 mass% water at 433 K for 3.6 ks. The insets are backscattered electron images of the cross-sections.

Fig. 3 Pore size distributions in the anodic films formed on titanium at 5 V and 20 V in 0.6 mol $dm^{-3}$ $K_2HPO_4$+0.2 mol $dm^{-3}$ $K_3PO_4$/glycerol electrolyte containing 0.04 mass% water at 433 K for 3.6 ks. The distributions were obtained from nitrogen adsorption isotherms at 77 K.

Fig. 4 GDOES depth profiles of the anodic films formed on titanium at (a) 5 V and (b) 20 V in 0.6 mol $dm^{-3}$ $K_2HPO_4$+0.2 mol $dm^{-3}$ $K_3PO_4$/glycerol electrolyte containing 0.04 mass% water at 433 K for 3.6 ks.

Fig. 5 Change in the thickness of the anodic oxide films with electric charge passed during anodizing titanium at 5 and 20 V in 0.6 mol $d^{-3}$ $K_2HPO_4$+0.2 mol $dm^{-3}$ $K_3PO_4$ glycerol electrolyte containing 0.04 mass% water at 433 K.

Fig. 6 X-ray diffraction patterns of titanium specimens anodized at 5 and 20 V in 0.6 mol $dm^{-3}$ $K_2HPO_4$+0.2 mol $dm^{-3}$ $K_3PO_4$ glycerol electrolyte containing 0.04 mass% water at 433 K for 3.6 ks.

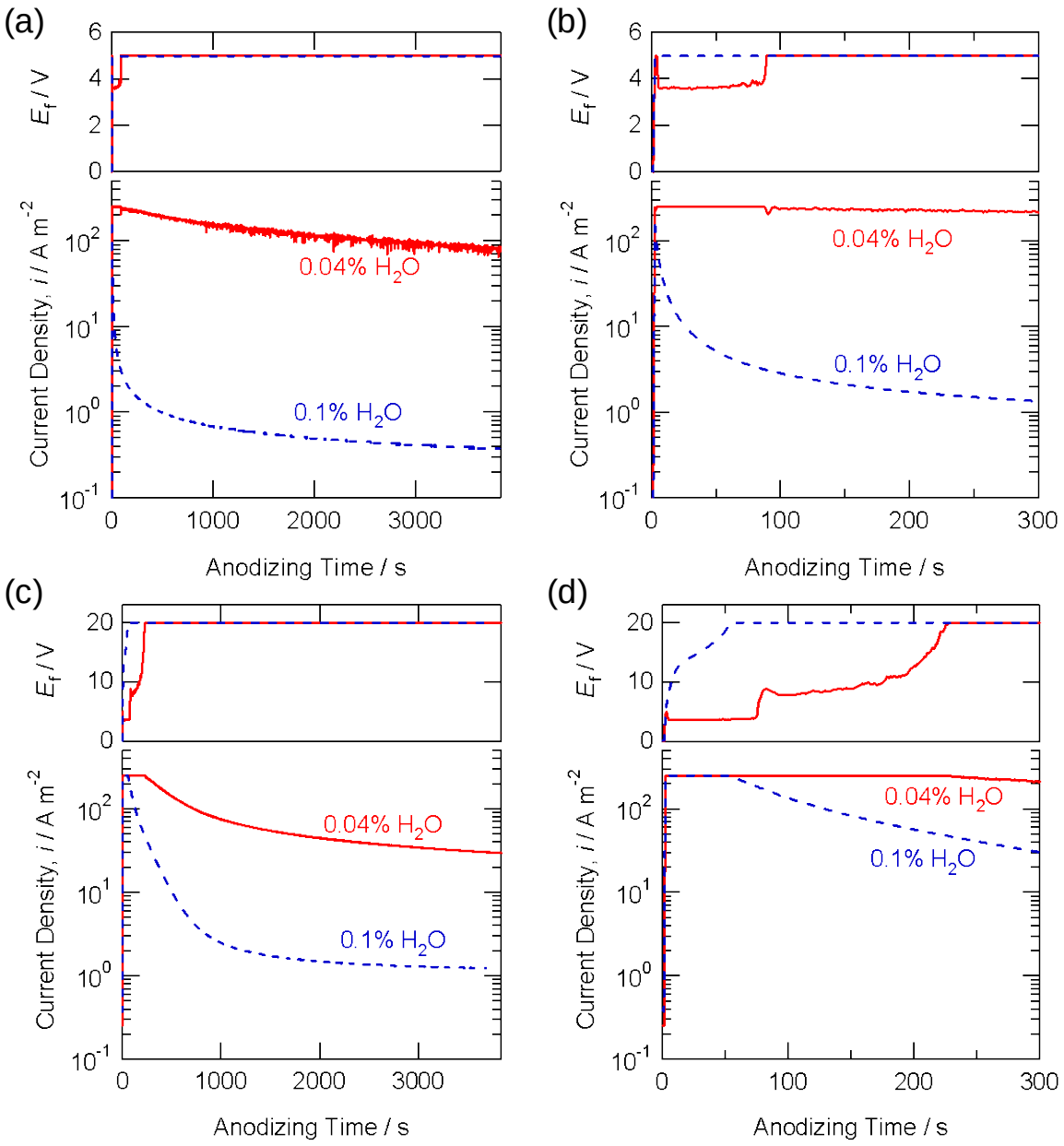


Fig. 1 Voltage-time and current-time responses of titanium during anodizing at (a), (b) 5 V and (c), (d) 20 V in 0.6 mol d$^{-3}$ $K_2HPO_4$+0.2 mol dm$^{-3}$ $K_3PO_4$ glycerol electrolytes containing 0.04 and 0.1 mass% water at 433 K for 3.6 ks. Constant current density of 250 A m$^{-2}$ was applied before reaching the selected voltages.

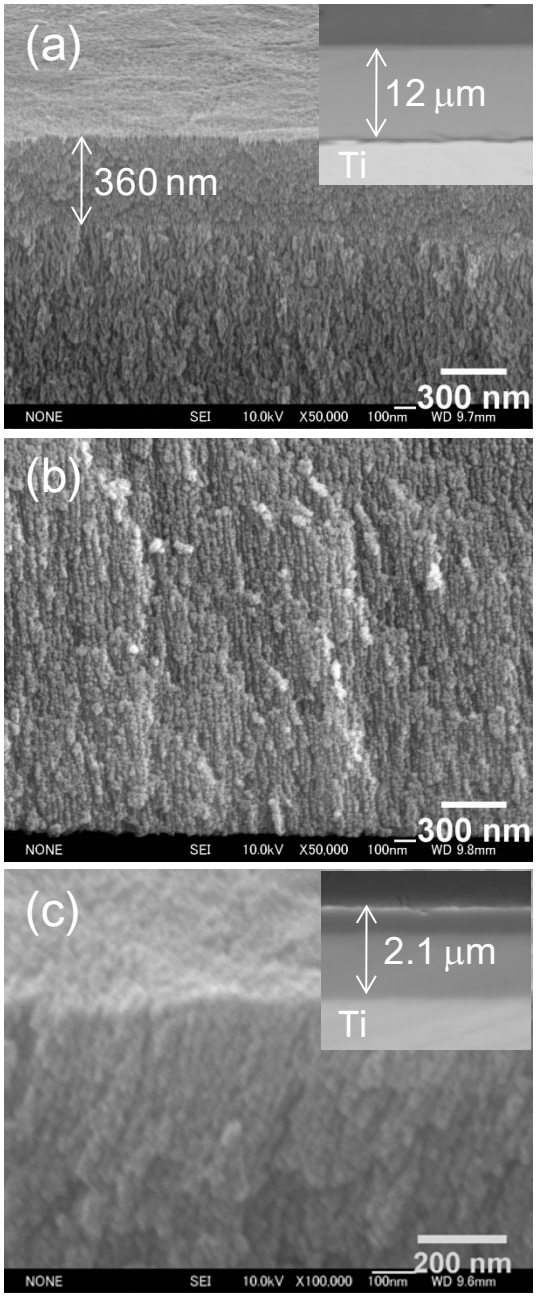


Fig. 2 Scanning electron micrographs of fractured cross-sections of the anodic films formed on titanium at 5 V (outer part (a) and inner part (b)) and 20 V (outer part (c)) in 0.6 mol $d^{-3}$ $K_2HPO_4$+0.2 mol $dm^{-3}$ $K_3PO_4$ glycerol electrolyte containing 0.04 mass% water at 433 K for 3.6 ks. The insets are backscattered electron images of the cross-sections.

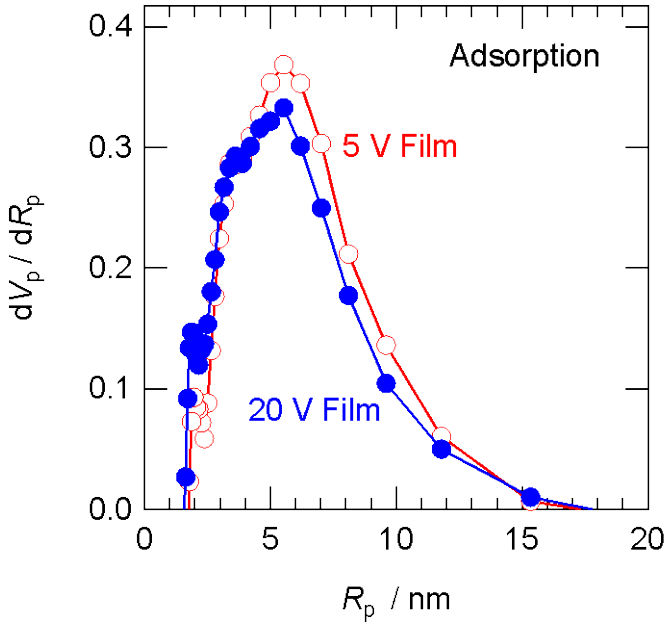


Fig. 3 Pore size distributions in the anodic films formed on titanium at 5 V and 20 V in 0.6 mol $dm^{-3}$ $K_2HPO_4$+0.2 mol $dm^{-3}$ $K_3PO_4$ glycerol electrolyte containing 0.04 mass% water at 433 K for 3.6 ks. The distributions were obtained from nitrogen adsorption isotherms at 77 K.

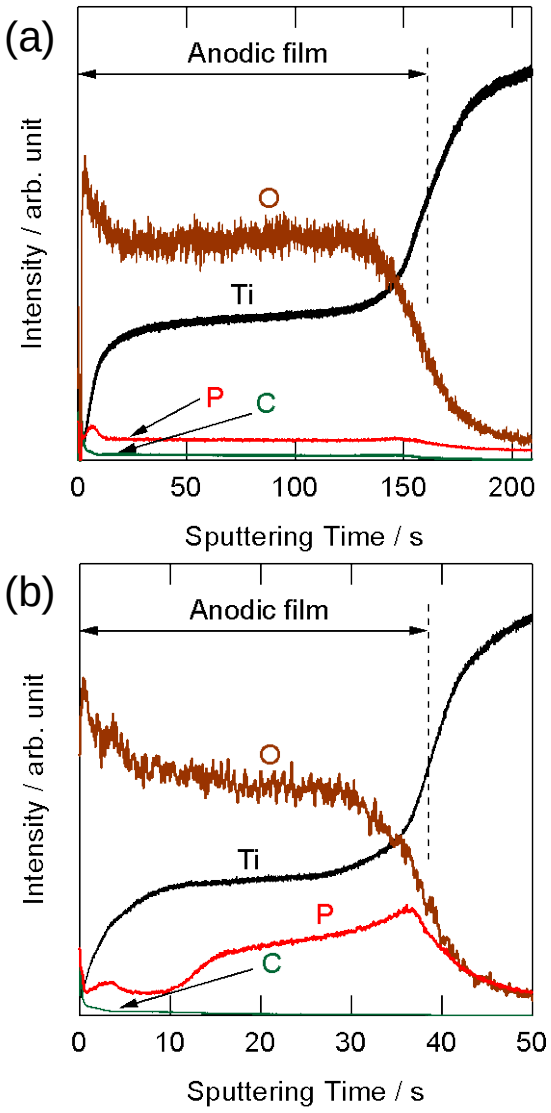


Fig. 4 GDOES depth profiles of the anodic films formed on titanium at (a) 5 V and (b) 20 V in 0.6 mol $dm^{-3}$ $K_2HPO_4$+0.2 mol $dm^{-3}$ $K_3PO_4$ glycerol electrolyte containing 0.04 mass% water at 433 K for 3.6 ks.

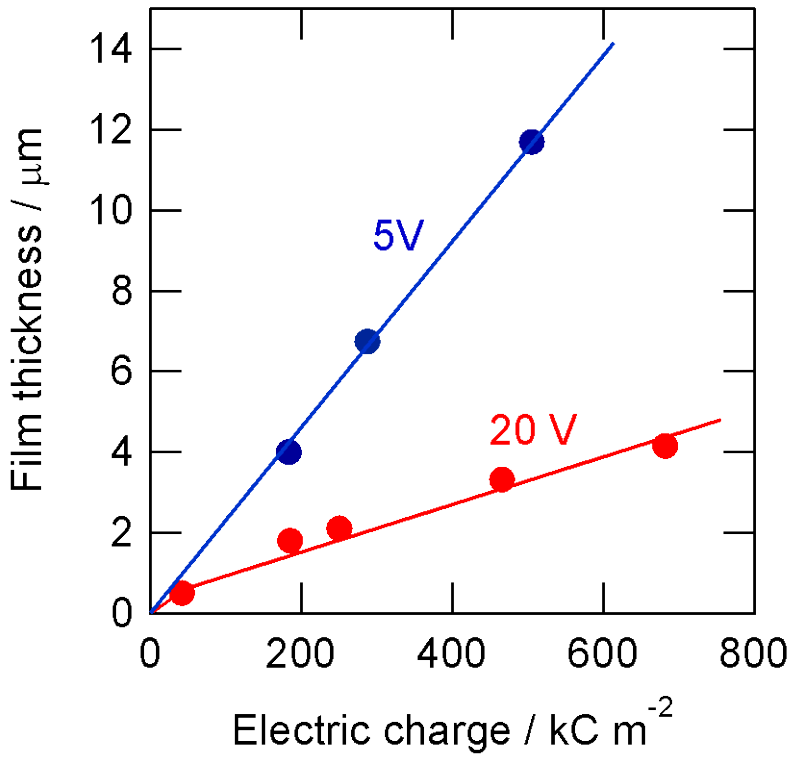


Fig. 5 Change in the thickness of the anodic oxide films with electric charge passed during anodizing titanium at 5 and 20 V in 0.6 mol $d^{-3}$ $K_2HPO_4$+0.2 mol $dm^{-3}$ $K_3PO_4$ glycerol electrolyte containing 0.04 mass% water at 433 K.

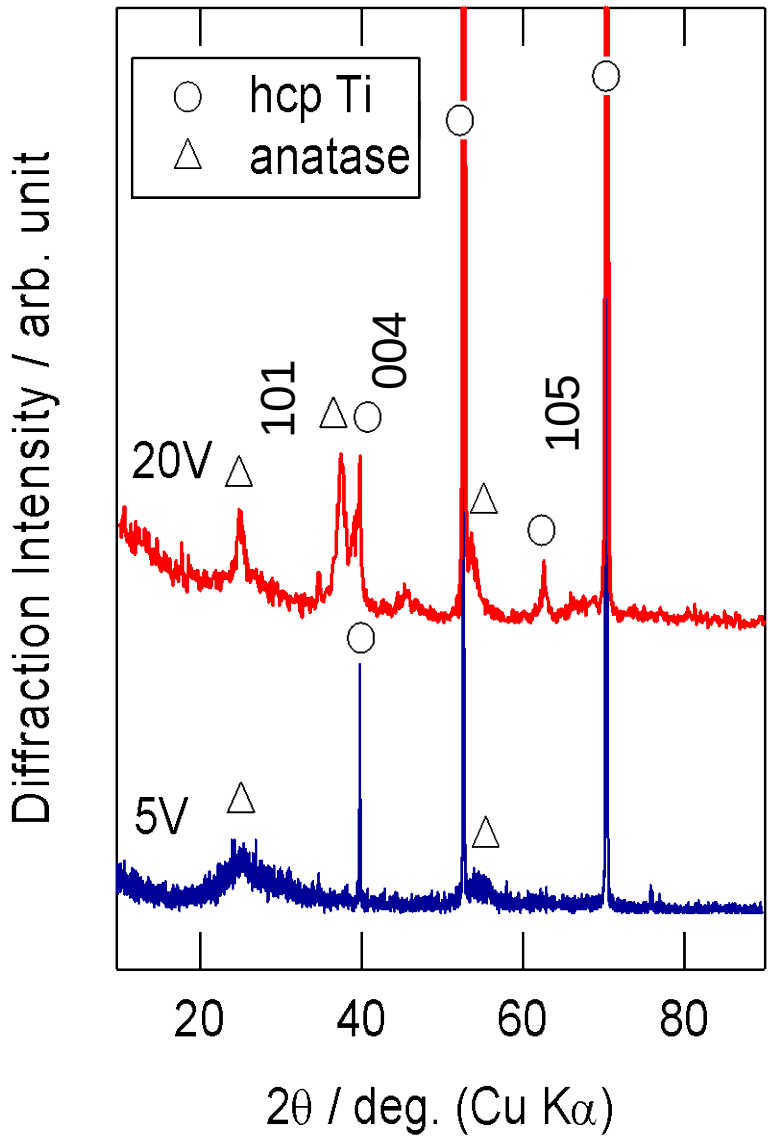


Fig. 6 X-ray diffraction patterns of titanium specimens anodized at 5 and 20 V in 0.6 mol $dm^{-3}$ $K_2HPO_4$+0.2 mol $dm^{-3}$ $K_3PO_4$ glycerol electrolyte containing 0.04 mass% water at 433 K for 3.6 ks.